Journal of the Physical Society of Japan
Vol. 76, No. 11, November, 2007, 111013

Physics at LHC

Shoji ASAI

Department of Physics, University of Tokyo, Tokyo 113-0033

(Received March 30, 2007; accepted September 5, 2007; published November 12, 2007)

Physics potential of the LHC (Large Hadron Collider) is summarized in this report, focusing especially on two major topics, the Higgs boson and Supersymmetry. ATLAS and CMS collaborations have excellent potential to discover them, if they exist at the mass scale less than about 1 and 3 TeV, respectively. Methods and their expected performances, to determine the properties of these new particles, are summarized.

KEYWORDS: LHC, collider, ATLAS, Higgs, SUSY
DOI: 10.1143/JPSJ.76.111013

1. Introduction

The most urgent and important topics of contemporary particle physics are (1) to understand *the origin of "Mass"* (the Electroweak symmetry braking) and (2) to discover of *the physics beyond the Standard model (SM)*. These are the main purpose of the Large Hadron Collider (LHC),[1] in which two protons collide with the center-of-mass energy of 14 TeV. The first physics collision is expected in the summer of 2008 with the lower luminosities of about $10^{32}\,\mathrm{cm^{-2}\,s^{-1}}$. The design luminosity of $10^{34}\,\mathrm{cm^{-2}\,s^{-1}}$, which corresponds to $100\,\mathrm{fb^{-1}}$ per year, will be achieved within several years.

The production cross-sections of the various high p_T and high mass elementary processes are expected to be large at LHC, since gluon inside protons can contribute remarkably. Furthermore, because the LHC provides the high luminosity of 10–$100\,\mathrm{fb^{-1}}$ per year, large numbers of the interesting events will be observed as summarized in Table I. LHC has an excellent potential to produce high mass particles, for example, the top quark, the Higgs boson and SUSY particles. I focus on the Higgs and Supersymmetry in this note, and refer to new gauge symmetry and extra space-dimensions only briefly as alternatives.

2. Detectors

Two general-purpose experiments have been constructed, ATLAS[2] and CMS,[3] at the LHC. The ATLAS (A Toroidal LHC Apparatus) detector is illustrated in Fig. 1, and it measures 22 m high, 44 m long, and weights 7,000 tons. The characteristics of the ATLAS detector are summarized as follows:[4]

- Precision inner tracking system is made with pixel, strip of silicon and TRT (Transition Radiation Tracker) with 2 T solenoid magnet. Good performance is expected on the B-tagging and the γ-conversion tagging.
- Liquid argon electromagnetic calorimeter has fine granularity for space resolution, and longitudinal segmentation to obtain fine angular resolution and excellent particle identifications. It has also good energy resolution of about 1.3% for 100 GeV $e^{\pm}$ and γ.
- Large muon spectrometer with air core toroidal magnet will provide a precise measurement on muon momenta (about 2% for 100 GeV-$\mu^{\pm}$) even in the forward region.

Table I. Production cross-section and event numbers for major high p_T and high mass processes with an integrated luminosity of $10\,\mathrm{fb^{-1}}$.

	σ (pb)	Event number at LHC ($L = 10\,\mathrm{fb^{-1}}$)
$W^{\pm} \to \ell^{\pm}\nu$	6.0×10^4	$\sim 10^9$
$Z^0 \to \ell^+\ell^-$	5.7×10^3	$\sim 10^8$
$t\bar{t}$	830	$\sim 10^7$
jj $p_T > 200$ GeV	10^5	$\sim 10^9$
SM Higgs (M = 115 GeV)	35	$\sim 10^5$
$\tilde{g}\tilde{g}$ (M = 500 GeV)	~ 100	$\sim 10^6$
(M = 1 TeV)	~ 3	$\sim 10^4$

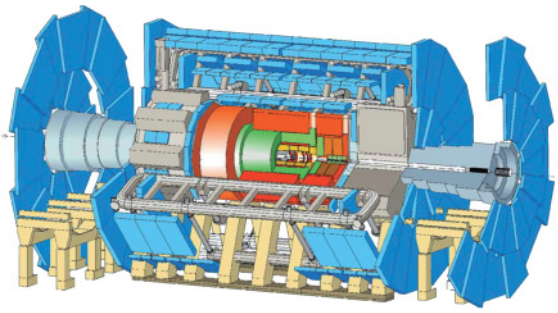

Fig. 1. Overall layout of the ATLAS detector. Outside blue parts are the muon system. Red and green parts are hadron and EM calorimeters, respectively. Inner tracking system is installed inside the EM calorimeter.

The CMS (Compact Muon Solenoid) detector (Fig. 2) measures 15 m high, 21 m long, and weights 12,500 tons, with the following features:[5]

- Precise measurement of the high p_T track is performed with 4 T solenoid magnet.
- $PbW0_4$ crystal electromagnetic calorimeter has an excellent energy resolution of 0.9% for 100 GeV $e^{\pm}$ and γ.

3. Higgs Physics

A discovery of one or several Higgs bosons will give a definite experimental proof of the breaking mechanism of the Electroweak gauge symmetry, and detail studies of the Yukawa couplings between the Higgs boson and various

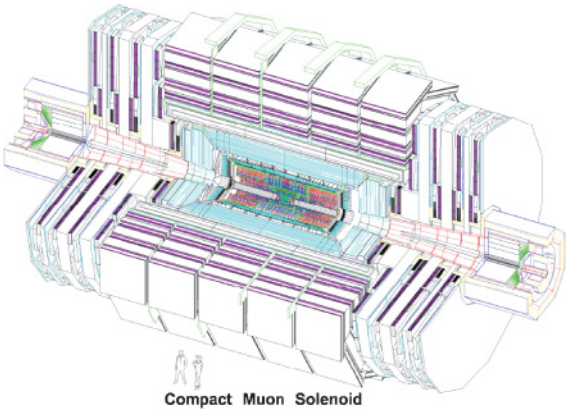

Fig. 2. Overall layout of the CMS detector. Outside white and magenta parts are the magnetic return yoke (iron) and the muon detectors. Light blue and blue show the hadron and EM calorimeters, respectively. Inner tracking system is installed inside the EM calorimeter and 4 T solenoid magnet is installed outside of the hadron calorimeter.

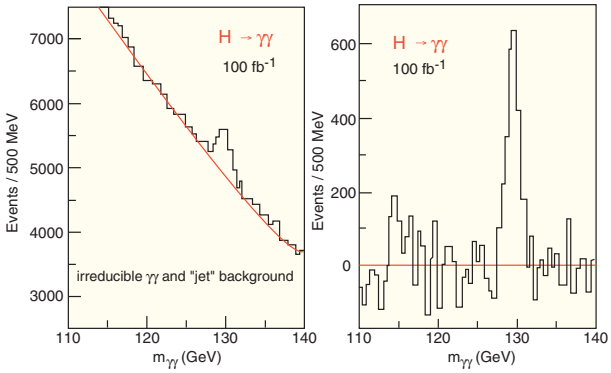

Fig. 3. The invariant mass distribution of $\gamma\gamma$ ($L = 100\,fb^{-1}$ at CMS). H^0_{SM} mass is assumed to be 130 GeV. The left figure shows signal plus background events, and the right one shows the subtracted spectrum. In addition to the irreducible $\gamma\gamma$ background, there are jet–γ and jet–jet background events, in which a jet is misidentified as a photon.

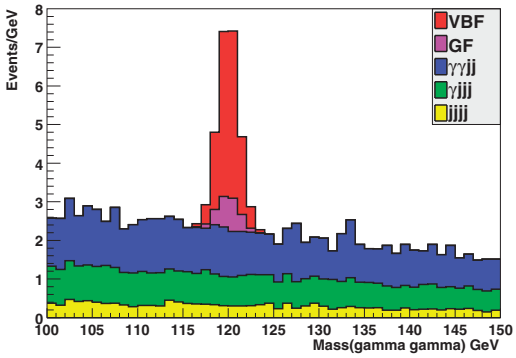

Fig. 4. The invariant mass distribution of $\gamma\gamma$ with two high p_T forward jets ($L = 30\,fb^{-1}$ at ATLAS Preliminary). $M(H^0_{SM}) = 120$ GeV is assumed, and fake background processes, in which a jet is misidentified as a photon, are also shown in the green and yellow histograms.

fermions will give insights on the origin of lepton and quark masses. The mass of the SM Higgs boson itself is not theoretically predicted, but it's upper limit is considered to be about 1 TeV from the unitary bound of the W^+W^- scattering amplitudes, or even 200 GeV (95% C.L.) from the Electroweak precision measurements.[6] The lower limit of the Higgs boson mass is set at 114 GeV (95% C.L.) by the direct searches at LEP. The Higgs boson should exist in the narrow mass range of 114–200 GeV, and lighter than 130–150 GeV if the Supersymmetry exists.

The SM Higgs boson, H^0_{SM}, is produced at the LHC predominantly via gluon–gluon fusion (GF)[7] and the second dominant process is vector boson fusion (VBF).[8] The production cross-sections are summarized in the report.[9] H^0_{SM} decays[10] mainly into $b\bar{b}$ and $\tau^+\tau^-$ for the lighter case ($\lesssim$130 GeV). On the other hand, it decays into W^+W^- and ZZ with a large branching fraction for the heavier case ($\gtrsim$140 GeV). Although its decay into $\gamma\gamma$, via the one-loop process including top quark or W boson, is suppressed ($\sim 2 \times 10^{-3}$), this decay mode is very important at the LHC.

3.1 $H^0_{SM} \to \gamma\gamma$ in GF and VBF

Although the branching fraction of this decay mode is small and there is a large background processes via $q\bar{q} \to \gamma\gamma$, the distinctive features of the signal, high p_T isolated two photons with a mass peak, allows us to separate the signal from the large irreducible background. Both the ATLAS[4] and CMS[5] detectors have excellent energy and position resolutions for photon, and the mass resolution of the $H^0_{SM} \to \gamma\gamma$ process is expected to be 1.3 GeV (ATLAS[11]) and 0.9 GeV (CMS[12]). Sharp peak appears at Higgs boson mass over the smooth distribution of background events as shown in Fig. 3. This channel is promising for the light Higgs boson, whose mass is lighter than 140 GeV, and this mode indicates the spin of the Higgs boson candidate.

VBF provides additional signatures in which two high p_T jets are observed in the forward regions, and only the two photons from the decay of H^0_{SM} will be observed in the wide rapidity gap between these jets. The rapidity gap (no jet activity in the central region) is expected because there is no color-connection between two out-going quarks. These signatures suppress the background contributions significantly and improve the signal-to-noise ratio as shown in Fig. 4. Although the signal statistics is limited, the background contributions are dramatically suppressed and the distribution of the background becomes flat. A significance of about 4.5 σ is obtained from VBF processes with a integrated of $30\,fb^{-1}$ it gains a significance of the inclusive $H^0_{SM} \to \gamma\gamma$ analysis.

3.2 $H^0_{SM} \to \tau^+\tau^-$ in VBF

$H^0_{SM} \to \tau^+\tau^-$ provides high p_T $\ell^\pm$, when τ decays leptonically, and it can makes a clear trigger. Momenta carried by ν's emitted from τ decays can be solved approximately by using the $\not{E}_T$ information,[13] and the Higgs mass can be reconstructed.[14] Figure 5 shows the mass distributions of the reconstructed tau-pair. The mass resolutions of about 10%[15] can be achieved, and the signal can be separated from the Z-boson production background. The performance of the $\not{E}_T$ measurement is crucial in this analysis as the same as in the SUSY search. We can obtain a significance of about 4 σ for this channel[15] for $m_{H^0_{SM}} < 130$ GeV with a luminosity of $10\,fb^{-1}$, and also this channel provides a direct information on the coupling between the Higgs boson and a fermion, the tau lepton.

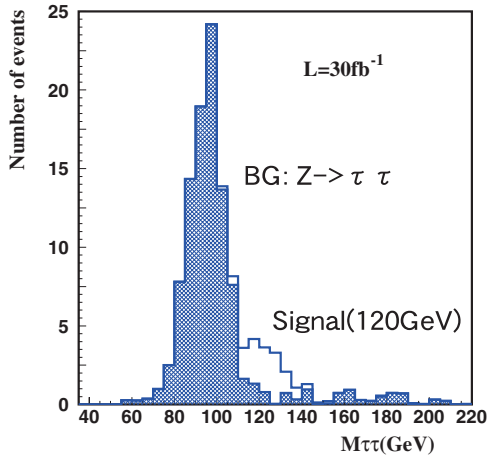

Fig. 5. The invariant mass distribution of $\tau^+\tau^-$ with high p_T forward jets ($L = 30\,fb^{-1}$ at ATLAS). One tau decays leptonically and another decays hadronically in this analysis. Open histogram shows the signal with $M(H^0_{SM}) = 120\,GeV$. The similar significance is obtained when both taus decay into leptons.

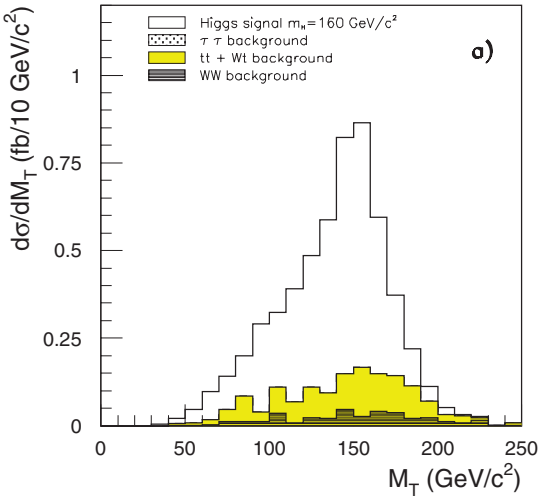

Fig. 7. The transverse mass distribution of $\not{E}_T$ and $\ell^+\ell^-$, in which $M(H^0_{SM}) = 160\,GeV$ is assumed (ATLAS). Open histogram shows the Higgs signal and the hatched histogram show the background processes ($t\bar{t}$ and W^+W^-).

3.3 H^0_{SM} ($\rightarrow ZZ \rightarrow \ell^+\ell^-\ell^+\ell^-$) *in GF*

Dominant decay modes of the heavier H^0_{SM} are ZZ and W^+W^-. The four-lepton channel ($H^0_{SM} \rightarrow ZZ \rightarrow \ell^+\ell^-\ell^+\ell^-$) is very clean and called "the gold-plated". Although the branching fraction of $ZZ \rightarrow \ell^+\ell^-\ell^+\ell^-$ is small, a sharp mass peak is expected as shown in Fig. 6, if the Higgs boson is heavier than 140 GeV. Mass resolution of the four lepton system is typically 1%.[11,12] As shown in Fig. 6, the main background process is ZZ production, which gives continuous distribution above 200 GeV. Small contaminations come from $t\bar{t}$ and $Z^0b\bar{b}$, in which semi-leptonic decays of bottom quark are identified as isolated leptons. In order to reduce these contaminations, leptons are required to be well isolated from hadron activities and their track impact parameters should be consistent with zero. The $\ell^+\ell^-\ell^+\ell^-$ channel has a good performance in the wide mass range from 130 to 800 GeV, except around 170 GeV, where the W^+W^- is the dominate decay mode.

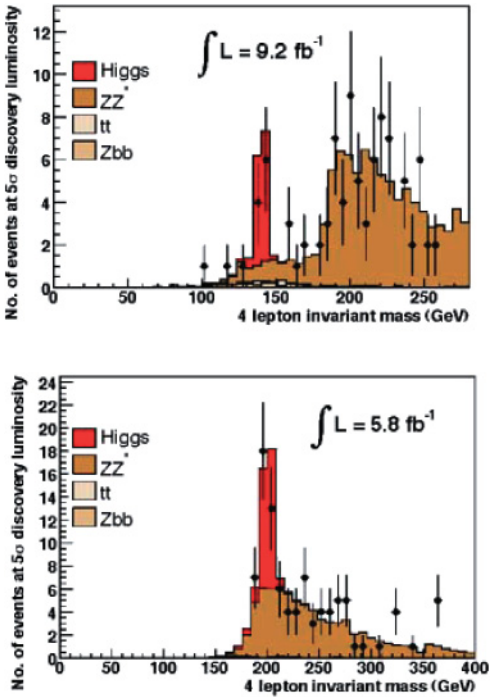

Fig. 6. The invariant mass distributions of $\ell^+\ell^-\ell^+\ell^-$ for $M(H^0_{SM}) = 140$ (upper) and 200 (lower) GeV with luminosities of 9.2 and $5.8\,fb^{-1}$, respectively (CMS). With these luminosities, a significance of 5σ is obtained.

3.4 H^0_{SM} ($\rightarrow W^+W^- \rightarrow \ell^\pm\nu\ell^\pm\nu$) *in VBF*

When the Higgs mass is around 170 GeV, the branching fraction of $H^0_{SM} \rightarrow W^+W^-$ is almost 100%. The whole mass range of 130–200 GeV is well covered by the analysis of VBF $H^0_{SM} \rightarrow W^+W^- \rightarrow \ell^+\nu\ell^-\nu$. The transverse mass, M_T, is defined as $\sqrt{2\,\not{E}_T P_T(\ell^+\ell^-)(1-\cos\phi)}$, in which ϕ is the azimuthal angle between the $\not{E}_T$ and $P_T(\ell^+\ell^-)$. Figure 7 shows the M_T distribution and a clear Jacobian peak is observed above smooth background distributions. The main background process is $t\bar{t}$, and this can be suppressed by using the azimuthal angle correlation between the dileptons. Since the Higgs boson is a spin zero particle, the helicities of the emitted W bosons are opposite. The leptons are then emitted preferably in the same direction due to the 100% Parity violation in W decays.

3.5 *Overall discovery potential of* H^0_{SM}

Discovery potential of H^0_{SM} are summarized in Fig. 8 as a function of the Higgs mass with an integrated luminosity of $10\,fb^{-1}$. $H^0_{SM} \rightarrow \gamma\gamma$ in GF and VBF and $\tau^+\tau^-$ channels have good potential in the mass region lighter than 130 GeV. For the heavy mass case (≥ 130 GeV), decay to ZZ ($\rightarrow \ell^+\ell^-\ell^+\ell^-$) and W^+W^- have an excellent performance even above 10σ. When both ATLAS and CMS significances are combined, we can perform to discover (5σ C.L.) and exclude (98% C.L.) the Higgs boson up to 1 TeV mass with the integrated luminosities of 5 and $1\,fb^{-1}$, respectively. Therefore the crucial test of the Higgs mechanism of the symmetry braking can be performed within 2009.

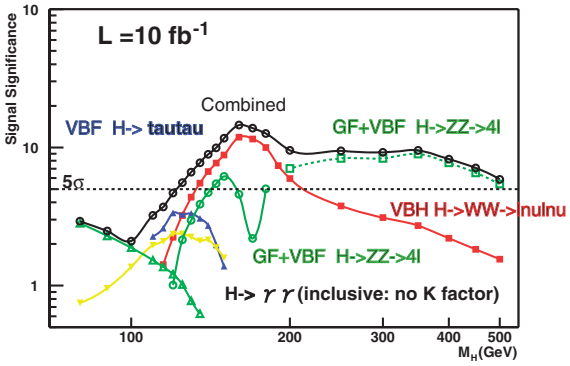

Fig. 8. The H^0_{SM} discovery potential with $L = 10\,fb^{-1}$ in the various modes (ATLAS). The horizontal axis shows the mass of Higgs boson, and the vertical gives the significance of the Higgs signal. Open black circles show the combined performance of all the modes. The horizontal dotted line shows the 5σ discovery level. The exclusive analysis of Fig. 4 is not yet combined.

3.6 *Measurement of mass and couplings of the Higgs boson*

Measurements on the properties of the discovered Higgs boson give further insights to the origin of masses. Higgs mass can be measured precisely in $H^0_{SM} \to \gamma\gamma$ and $H^0_{SM} \to ZZ\,(\to \ell^+\ell^-\ell^+\ell^-)$. Accuracy of less than 0.2% error can be achieved with $L = 300\,fb^{-1}$, if the mass is smaller than 500 GeV. When the Higgs boson is heavier than 500 GeV, the resonance becomes too broad, and the precision becomes worse.

Measurements of the couplings between the Higgs boson and fermions/Gauge bosons will give the direct informations of the origin of "Mass", and fermion's couplings will give the first evidence of Yukawa couplings. Figure 9 shows the accuracy of the coupling measurements between the Higgs boson and fermion/Gauge bosons. We can measure without an assumption the relative magnitudes of the couplings normalized to the coupling between the W and the Higgs boson. We can determine the coupling between the Z and the Higgs boson precisely, where the accuracy of 5–10% can be achieved in all the mass region. Couplings between the Higgs and the 3rd generation fermions (top and tau) are determined with accuracies of 10–15%, but can not determine well for the bottom quark.

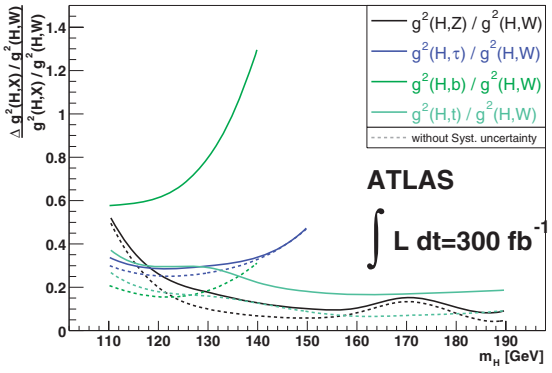

Fig. 9. Relative precision of the H^0_{SM} coupling squared as a function of the Higgs mass. Luminosity of $300\,fb^{-1}$ is assumed. Solid lines shown the results including the systematic errors.

4. Supersymmetry

Supersymmetric (SUSY) standard models[16] are most promising extensions of the SM, because the SUSY can naturally explain the weak boson mass scale. Furthermore, the SUSY models provide a natural candidate of the cold dark matter,[17] and they have given a hint of the Grand Unification in which three gauge couplings of the SM are unified at around 2×10^{16} GeV. In these theories, each elementary particle has a superpartner whose spin differs by 1/2 from that of the particle. Discovery of the SUSY particles should open a new epoch of the fundamental physics, which is another important purpose of the LHC project.

4.1 *Introduction of Super-Gravity model*

There are, in general, more than 100 free parameters to describe soft SUSY breaking,[16] but there are strong constraints among them from the smallness of the flavor-changing neutral current. Among various models of the SUSY breaking that can naturally satisfy these constraints, Super-Gravity model,[18] Gauge-mediated model,[19] and Anomaly-mediated model[20] are predictable and promising. Performance of the ATLAS experiments based on the Super-Gravity model is summarized in this section.

Minimal Super-Gravity Model (mSUGRA)[18] is a special case of the Minimal Supersymmetric Model (MSSM), in which the soft SUSY breaking terms are assumed to be communicated from the SUSY breaking sector by gravity only and that these terms are universal at the GUT scale. There are only five free parameters in this model; m_0 (universal mass of all scalar particles at the GUT scale), $m_{1/2}$ (universal mass of all gauginos at the GUT scale), A_0 (common scale of trilinear couplings at the GUT scale), $\tan\beta$ ($\equiv v_2/v_1$) (ratio of VEV of two Higgs fields at the Electroweak scale) and the sign of μ (Higgsino mass term).

In this model, masses of supersymmetric particles are mainly determined by $m_{1/2}$ and m_0; $\tilde{g}$ becomes heavy due to large radiative corrections, and its mass is approximately 2.5 $m_{1/2}$ at the energy scale of the LHC. Higgsino mass ($|\mu|$) becomes larger than the weak Gaugino masses at the EW scale, except for the case of $m_0 \gg m_{1/2}$. Then the lighter states of the neutralinos, $\tilde{\chi}^0_1$ and $\tilde{\chi}^0_2$, become almost pure Bino- and Wino-states ($\tilde{\chi}^0_1 \sim \tilde{B}^0$, $\tilde{\chi}^0_2 \sim \tilde{W}^0$), and the lighter state of the charginos, $\tilde{\chi}^\pm_1$, is also Wino-like ($\tilde{\chi}^\pm_1 \sim \tilde{W}^\pm$). Scalar lepton masses are determined mainly by m_0 and sub dominantly by $m_{1/2}$. On the other hand, scalar quark masses depend on both m_0 and $m_{1/2}$. Here is a typical spectrum of the SUSY particles;

- $m(\tilde{g}) \sim 2.5\ m_{1/2}$.
- $m(\tilde{\chi}^0_1) \sim 0.4\ m_{1/2}$.
- $m(\tilde{\chi}^0_2) \sim m(\tilde{\chi}^\pm_1) \sim 0.8\ m_{1/2}$.
- $m(\tilde{\ell}^\pm_R) \sim \sqrt{m_0^2 + 0.15 m_{1/2}^2}$
- $m(\tilde{\ell}^\pm_L) \sim \sqrt{m_0^2 + 0.5 m_{1/2}^2}$
- $m(\tilde{q}_{L,R}) \sim \sqrt{m_0^2 + 6 m_{1/2}^2}$

Masses of the lighter state of third generation scalar fermions ($\tilde{t}_1$, $\tilde{b}_1$, and $\tilde{\tau}_1$) depend also on A and $\tan\beta$,[21] and they are generally lighter than the first and second generation scalar fermions because of the following two reasons. Firstly, one loop radiative corrections due to their Yukawa

	$m(\tilde{g}) < m(\tilde{q})$	$m(\tilde{g}) \approx m(\tilde{q})$	$m(\tilde{g}) < m(\tilde{q})$
$\tilde{g}$	$q\bar{q}\tilde{B}^0$ ($\approx$1/7) $\tilde{g} \to q\bar{q}\tilde{W}^0$ ($\approx$2/7) $q\bar{q}\tilde{W}^\pm$ ($\approx$4/7)	$\tilde{g} \to t\tilde{t}_1$ $b\tilde{b}_1$	$\tilde{g} \to q\tilde{q}$
$\tilde{q}_L$	$\tilde{q}_L \to q\tilde{g}$	$\tilde{q}_L \to q\tilde{W}^0$ ($\approx$1/3) $q\tilde{W}^\pm$ ($\approx$2/3)	
$\tilde{q}_R$	$\tilde{q}_R \to q\tilde{g}$	$\tilde{q}_R \to q\tilde{B}^0$	

Fig. 10. Summary of decays of the colored Sparticles: Bino/Wino-eigenstates presented in the table can be regarded as mass-eigenstates, ($\tilde{B}^0 \sim \tilde{\chi}_1^0$, $\tilde{W}^0 \sim \tilde{\chi}_2^0$, and $\tilde{W}^\pm \sim \tilde{\chi}_1^\pm$), when m_0 is not too larger than $m_{1/2}$. In this case, Higgsino mass ($|\mu|$) becomes much larger than gaugino masses at the EW scale, and the Higgsino component decouples from the lighter mass-eigenstates as explained in the text.

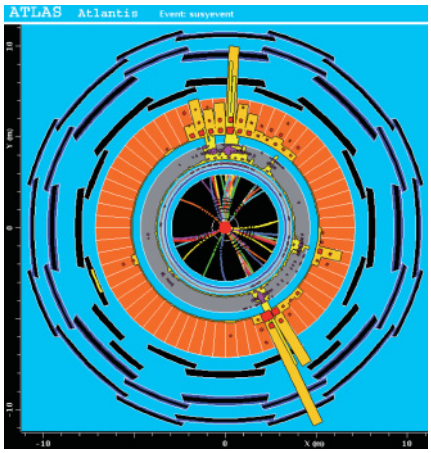

Fig. 11. Expected SUSY signal (simulated with the ATLAS detector); $\tilde{g}$ and $\tilde{q}$ are associate-produced and the $\tilde{g}$ decays into a quark and a $\tilde{q}$. The central colored tracks show the observed charged particles, and the yellows towers in the gray and orange parts show the energies deposited in the EM and hadron calorimeters, respectively.

couplings are always negative. Secondly, the supersymmetric partners of the right- and left-handed states mix, and the resultant lower mass eigenstate becomes lighter. This mixing contribution depends on both A_0 and $\tan\beta$.

Dominant SUSY production processes at the LHC are $\tilde{g}\tilde{g}$, $\tilde{g}\tilde{q}$, and $\tilde{q}\tilde{q}$ through the strong interaction. These production cross-sections, σ, do not strongly depend on the SUSY parameters except for the masses of $\tilde{g}$ and $\tilde{q}$.[22] When their masses are lighter than 1 TeV, $\tilde{g}\tilde{g}$ is the main production process, and the total SUSY production cross-section, $\sigma(\tilde{g}\tilde{g}$, $\tilde{g}\tilde{q}$, and $\tilde{q}\tilde{q})$, is about 100 pb for $m_{\tilde{q}} = m_{\tilde{g}} = 500$ GeV, and 3 pb for 1 TeV. Even when their masses are 2 TeV, sizable production cross-section of about 20 fb is expected. $\tilde{u}\tilde{u}$ and $\tilde{u}\tilde{d}$ are the main production processes for such a heavy case, since u and d quarks are the valence quarks of the incoming protons.

Decay modes of $\tilde{g}$ and $\tilde{q}$ are controlled by the mass-relation between each other, and are summarized in Fig. 10. If kinematically possible, they decay into 2-body through the strong interactions. Otherwise, they decay into an electroweak gaugino plus quark(s).

4.2 *Event topologies of SUSY events and discovery potential*

$\tilde{g}$ and/or $\tilde{q}$ are copiously produced at the LHC. High p_T jets are emitted from the decays of $\tilde{g}$ and $\tilde{q}$ as presented in Fig. 10. If the R-parity[23] is conserved, each event contains two $\tilde{\chi}_1^0$'s in the final state, which is stable, neutral and weakly interacting and escapes detection. This $\tilde{\chi}_1^0$ is an excellent candidate of the cold dark matter. The missing transverse energy ($\not{E}_T$), which is carried away by the two $\tilde{\chi}_1^0$'s, plus multiple high p_T jets is the leading experimental signature of the SUSY at the LHC. Additional leptons, $\tau^\pm$ (decaying hadronically) and h ($\to b\bar{b}$), coming from the decays of $\tilde{\chi}_2^0$ and $\tilde{\chi}_1^\pm$, can also be detected in the some part of event. Typical simulated SUSY event is shown in Fig. 11 for the ATLAS detector.

Inclusive searches will be performed with the large $\not{E}_T$ and high p_T multi-jet topology (no-lepton mode). One additional hard lepton (one-lepton mode) or two same-sign (SS-dilepton) and opposite-sign leptons (OS-dilepton) can be added to the selections. These four are the promising modes of the SUSY searches.

The following four SM processes can potentially have $\not{E}_T$ event topology with jets:

- $W^\pm(\to \ell\nu)$ + jets,
- $Z^0(\to \nu\bar{\nu}, \tau^+\tau^-)$ + jets,
- $t\bar{t}$ + jets,
- QCD multi-jets with mis-measurement and semi-leptonic decays of $b\bar{b}$ and $c\bar{c}$ with jets

We require at least four jets with $p_T \geq 50$ GeV, and p_T of the leading jets and $\not{E}_T$ are required to be larger than 100 GeV. The azimuthal angles between $\not{E}_T$ and the leading three jets are required to be larger than 0.2 for the no-lepton mode to reduce the QCD background. Effective mass, $M_{eff} = \not{E}_T + \sum_{jets} p_T$, is a good variable to distinguish the signal from the background listed above. Excess coming from the SUSY signals can be clearly seen as shown in Fig. 12 for both no-lepton and one-lepton modes. $t\bar{t}$ is the dominant background process for the one-lepton mode, and all of the four processes listed above contribute to no-lepton mode. The QCD processes contribute only to the small $\not{E}_T$ and M_{eff}. The M_{eff} distribution has steeper slope for the SM background processes as shown in these figures. On the other hand, the distribution of the SUSY signals has a broad peak at large value (around 1.5 TeV in these figures), which is proportional to $\min(m(\tilde{g}), m(\tilde{q}))$.

The SM background contributions can be suppressed dramatically by requiring di-leptons as shown in Fig. 13. They show the $\not{E}_T$ distributions for the OS- and SS-dilepton modes, where $t\bar{t}$ is the dominant background process for both modes. Although the background contributions is seriously suppressed (the SS dilepton mode is the almost background free), the statistics of the SUSY signal is also typically a few % of no-lepton mode. Discovery potentials of dilepton modes are limited in the early stage of the collision, but these modes are important to reconstruct the decay chain mentioned later.

Figure 14 show the 5σ-discovery potential in the m_0–$m_{1/2}$ and the $m_{\tilde{q}}$–$m_{\tilde{g}}$ plane for $\tan\beta = 10$ with an integrated luminosity of 1 fb^{-1}. And the lowest shows the same figure

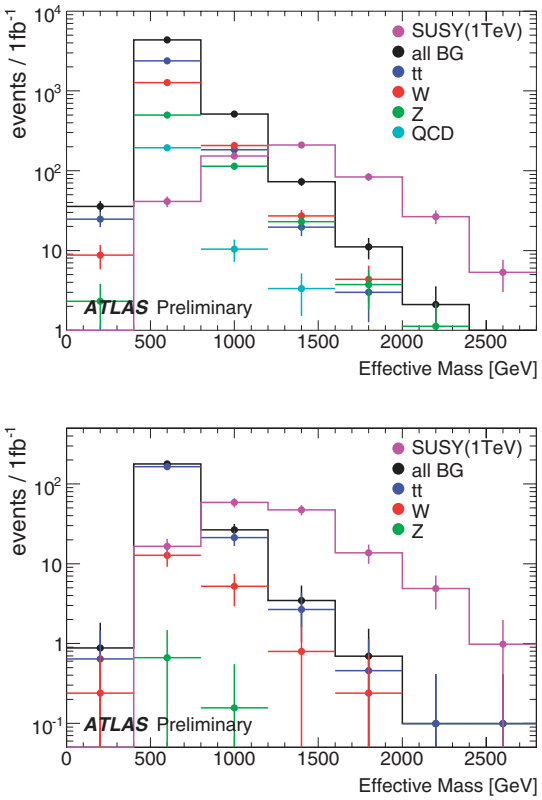

Fig. 12. Effective mass distributions of the SUSY signal and background processes with an integrated luminosity of $1\,\mathrm{fb}^{-1}$. Upper and lower figures show the no-lepton and one-lepton modes, respectively. Magenta histogram shows the SUSY signal, in which mass of squark and gluino are 1 TeV ($\tan\beta = 10$). The black histogram show the sum of all SM backgrounds. It includes the followings: $\mathrm{t\bar{t}}$ (blue), $\mathrm{W}^{\pm}$ + jets (red), Z^{0} + jets (green), and QCD jets (light blue). These results are obtained with the full simulation using GEANT4, in which all the materials in the detector are taken into account.

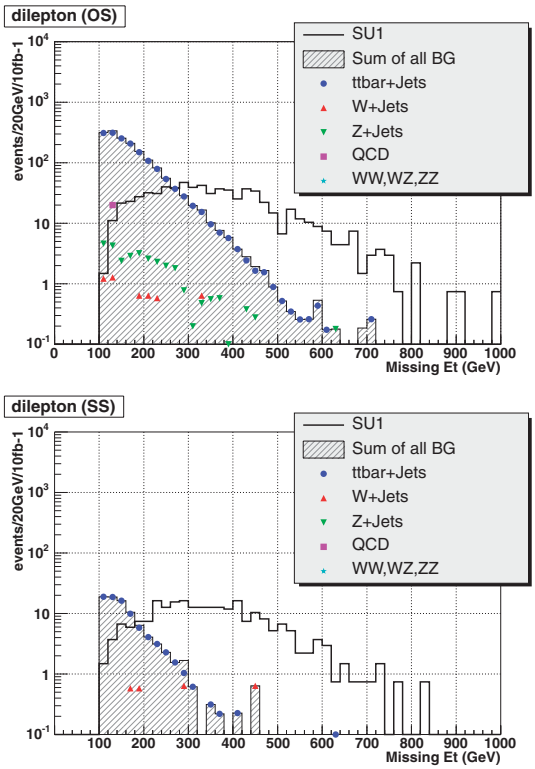

Fig. 13. Missing $\mathrm{E_T}$ distributions of the SUSY signal and background processes with a luminosity of $10\,\mathrm{fb}^{-1}$. Upper and lower figures show the Opposite–Sign-dilepton (OS) and the Same–Sign-dilepton (SS) cases, respectively. In both figures, the open histogram shows the SUSY signal for $m_0 = 70\,\mathrm{GeV}$, $m_{1/2} = 350\,\mathrm{GeV}$ and $\tan\beta = 10$. The hatched histogram shows the sum of all the SM backgrounds, while blue circles ($\mathrm{t\bar{t}}$) and green-triangles (Z^{0} + jets) show each component.

with an integrated luminosity of $30\,\mathrm{fb}^{-1}$. The results with three modes of no-lepton, one- and OS-dilepton are shown, and the hatched regions below each line show the systematic errors coming from the background estimations. The similar discovery potentials are obtained for no-lepton and one-lepton modes. As shown in these figures, $\tilde{\mathrm{g}}$ and $\tilde{\mathrm{q}}$ can be discovered up to the mass of $\sim$1.5 TeV with a luminosity of $1\,\mathrm{fb}^{-1}$, which corresponds to just one month run with $10^{33}\,\mathrm{cm}^{-2}\,\mathrm{s}^{-1}$. The discovery reach does not depend strongly on $\tan\beta$. The interesting region for the relic density of the dark matter is almost covered with just $1\,\mathrm{fb}^{-1}$. $\tilde{\mathrm{g}}$ and $\tilde{\mathrm{q}}$ can be discovered up to $\sim$2.5 TeV with a luminosity of $30\,\mathrm{fb}^{-1}$. $\tilde{\mathrm{g}}$ and $\tilde{\mathrm{q}}$, whose masses are about 2.7/3.0 TeV, can be discovered/excluded finally with a luminosity of $100\,\mathrm{fb}^{-1}$. This luminosity is corresponding to one year run with design luminosity ($10^{34}\,\mathrm{cm}^{-2}\,\mathrm{s}^{-1}$), and will be achieved in about 2011.

4.3 *Measurements of masses of SUSY particles*

Since two undetected LSP's exist in each event, there are six unknown momentum components in addition to the $\tilde{\chi}_1^0$ mass. No mass peak is expected in general. However it is possible to use kinematic end points of various distributions as follows.[11,24,25)]

- Select specific decay chain exclusively. For example,

$$\tilde{\mathrm{q}}_{\mathrm{L}} \to \tilde{\chi}_2^0 \mathrm{q} \to (\tilde{\ell}_R^{\pm}\ell^{\mp})\mathrm{q} \to ((\tilde{\chi}_1^0\ell^{\pm})\ell^{\mp})\mathrm{q}$$

- Make various distributions of invariant masses and p_{T}.
- Kinematic constraints are obtained from the end points of these distributions for the selected chain. These end points can be determined by the masses of the SUSY particles. SUSY events become background itself for detailed study, since there are many cascade decay patterns in $\tilde{\mathrm{q}}$ and $\tilde{\mathrm{g}}$. It is critical point that we can find out or not a useful decay-pattern in the SUSY events.

If there are three 2-body decay chains like the above example, which is a dominant mode in the parameter space of $m_0 \leq 0.8 m_{1/2}$, full reconstruction of masses is possible model-independently. The invariant mass distributions of $\ell\ell$, $\ell\ell$ + jet, and ℓ + jet can be calculated, and the three kinematic end points and one production threshold of the 4-body system ($\ell^+\ell^-\mathrm{q}\tilde{\chi}_1^0$) are obtained. On the other hand, there are four unknown masses ($\tilde{\mathrm{q}}_{\mathrm{L}}$, $\tilde{\chi}_2^0$, $\tilde{\ell}_R^{\pm}$, and $\tilde{\chi}_1^0$). Then all the four unknown masses can be determined model-independently. Although the errors of the determined masses are strongly correlated, accuracies of these masses are about 3–10% for $m(\tilde{\mathrm{q}}_{\mathrm{L}}) = 800\,\mathrm{GeV}$. Mass of the missing $\tilde{\chi}_1^0$ can be determined with an accuracy of about 10%, which is an extremely important result, since it can be the dark matter.

Reconstructions of the SUSY particle masses for the other decay-patterns are also possible[11,12,25)] by using the similar techniques. When we cannot identify a successive decay

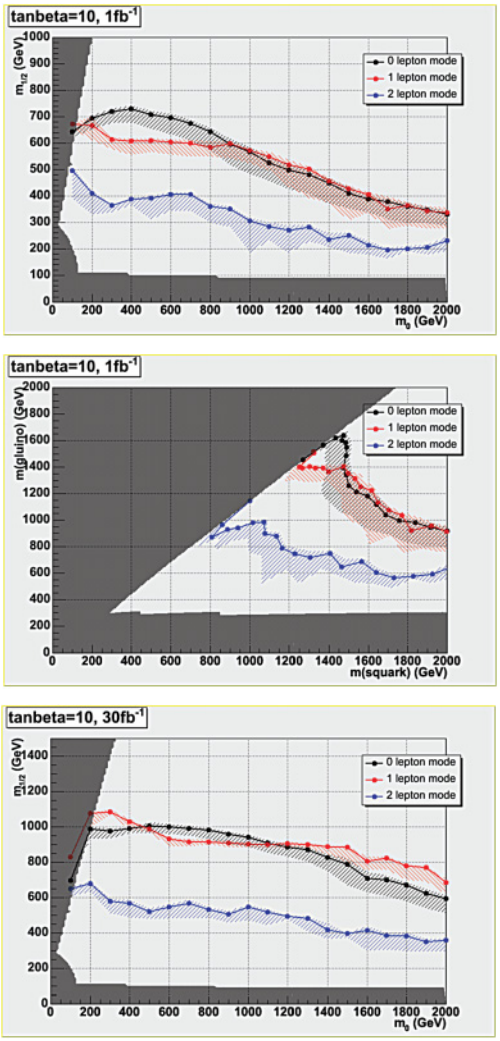

Fig. 14. 5σ-discovery potential (ATLAS preliminary) in the m_0–$m_{1/2}$ and $m_{\tilde{q}}$–$m_{\tilde{g}}$ planes: The upper two figures show the performance with $L = 1\,fb^{-1}$, and the lowest figure shows the results with $L = 30\,fb^{-1}$. In these figures, black, red and blue lines show the 5σ-discovery regions with no-lepton, one-lepton and OS-dilepton analyzes, respectively. The hatched region below each line shows the systematic uncertainty of the background estimations. Gray hatched regions are theoretically forbidden (no EWSB or slepton LSP).

chain listed above, the number of the observed constraints is less than that of the unknown masses. Therefore, some assumptions on SUSY breaking pattern are necessary to determine the mass spectrum. All the massed of $\tilde{g}$–$\tilde{q}_{L/R}$, $\tilde{\ell}^{\pm}$–$\tilde{\chi}^0_2$, and $\tilde{\chi}^0_1$ can determined within the assumed model, and we will be able to test various SUSY models by using these reconstructed mass spectra.[26)]

5. New Gauge Bosons

Many theories beyond the SM predict the existence of additional U(1) or SU(2) gauge groups and a discovery of new gauge bosons, Z′ and W′, should be its clear evidence of extension of the SM. Current mass limits on Z′ and W′ are about 800 GeV obtained at the Tevatron.

Z′ and W′ are produced with the Drell–Yan ($q\bar{q}$ annihilation) process at the LHC, and they decay into fermion pairs. Figure 15 shows the transverse mass distribution between the $\mu^{\pm}$ and $\not{E}_T$ momenta, $M_T = \sqrt{2P_T(\mu^{\pm})\,\not{E}_T(1-\cos\Delta\phi_{\mu\text{missing}})}$. Clear Jacobian peak will

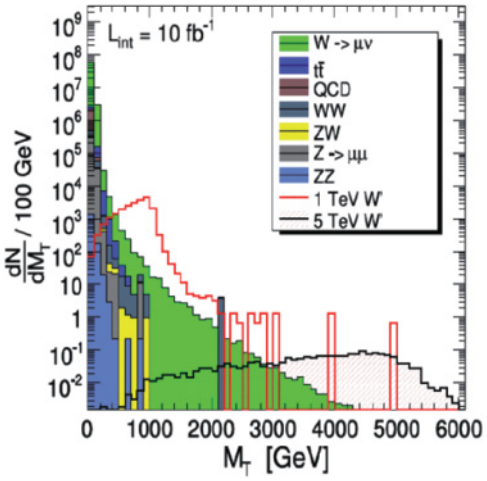

Fig. 15. Transverse mass distribution of $\mu^{\pm}$ and ν with $L = 10\,fb^{-1}$ (CMS): The steep green histogram shows the distributions of the $W^{\pm}$ background process. Red and black open histograms show the signal of W′ with mass of 1 and 5 TeV, respectively.

be observed at the mass of W′, and the background contribution is small in such a high M_T region. The results are obtained by assuming that the W′ coupling are the same as the $W^{\pm}$ coupling and no decay mode into new particles. The W′ can be discovered or excluded up to mass of 4.5 and 5 TeV, respectively[12)] with an integrated luminosity of $10\,fb^{-1}$, by combining the both $\mu\nu$ and $e\nu$ channels. $Z' \to \ell^+\ell^-$ makes a resonance peak in the high mass region, and Z′ can be discovered up to mass of 3.8 TeV with an integrated luminosity of $10\,fb^{-1}$.

6. Large Extra Space-Dimension and Black Holes

There is much recent theoretical interests that an extra-dimension exists in addition to the $3+1$ normal space–time dimensions, and it is compactified to the size of a few TeV, which is related to the true "Planck scale" of the complete theory. This new fundamental scale is denoted as "M_P". The idea is introduced as a possible solution of the hierarchy problem of the SM.[27)] The scatter processes at a few TeV scale should be treated within multi-dimensions, and the gravity interaction becomes as strong as the other interactions. For example, gravitons (G) are emitted in the hard scatter of $gg \to gG$ and escapes the detection. This makes an event with a single jet and large $\not{E}_T$ (monojet). We have the discovery-potential up to $M_P = 7$ TeV (additional dimension ≤ 3) with an integrated luminosity of $100\,fb^{-1}$.[12)]

If the true Plank scale is in the order of TeV, the Shwarzschild radius, R_s, is also sizable,

$$R_s = \frac{1}{\sqrt{\pi}M_P}\left[\frac{M_{BH}}{M_P}\left(\frac{8\Gamma\left(\frac{n+3}{2}\right)}{n+2}\right)\right]^{1/(1+n)}$$

for n extra space-dimensions. Mini black holes of a few TeV mass can be produced with parton–parton collisions within R_s at the LHC. Large production cross-section of order $\pi R_s{}^2 \sim 100\,pb$ is expected by classical arguments,[28)] the produced black hole decays through Hawking evaporation with the temperature:

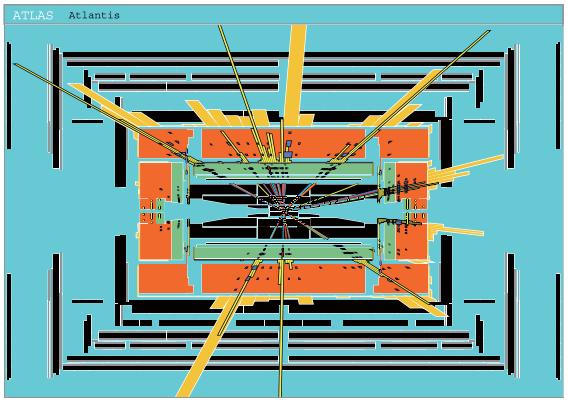

Fig. 16. Expected black hole signal with a mass of 5 TeV (simulated with ATLAS detector). The central colored tracks show the observed charged particles, and the yellows towers in the green and orange regions show the energies deposited in the EM and hadron calorimeters, respectively. Eleven energetic partons are emitted from the black hole decay.

$$T_H = M_{\mathrm{P}}\left[\frac{M_{\mathrm{P}}}{M_{\mathrm{BH}}}\frac{n+2}{8\Gamma\left(\frac{n+3}{2}\right)}\right]^{2/(n+1)}$$

As the produced black hole is heavier, the T_H becomes smaller (but still higher than 100 GeV), and many particles are emitted as shown in Fig. 16. These particles are energetic as the same orders of T_H. High p_{T} multi-particles are emitted spherically, and this event topology is quite different from the SM background processes. We can discover mini black holes up to mass of several TeV,[29] but we need more theoretical studies on the production and decay processes of the mini black holes at the LHC.

7. Summary

The LHC is the first experiment that probes directly physics at the TeV scale. The SM Higgs boson ($\mathrm{H}^0_{\mathrm{SM}}$) should be discovered with an integrated luminosity of 10 fb^{-1}, if it exists. $\mathrm{H}^0_{\mathrm{SM}} \to \gamma\gamma$ in GF (gluon fusion) and VBF (vector-boson fusion) and $\mathrm{H}^0_{\mathrm{SM}} \to \tau^+\tau^-$ in VBF are important processes for the Higgs lighter than 140 GeV. The decays into ZZ ($\to \ell^+\ell^-\ell^+\ell^-$) and $\mathrm{W}^+\mathrm{W}^-$ ($\to \ell\nu\ell\nu$) play important role if it is heavier. The Higgs boson mass can be determined precisely, and the couplings between Higgs and fermions/Gauge bosons can be measured with accuracies of about 5–20%. We can perform a critical test on the Higgs mechanism and will understand the origin of the elementary particle masses.

Supersymmetry should be discovered at the LHC, if gluino ($\tilde{\mathrm{g}}$) and squarks ($\tilde{\mathrm{q}}$) are lighter than about 2.7 TeV. Signals will be found not only in the ($\not{E}_{\mathrm{T}}$ + jets) channel but also in [$\not{E}_{\mathrm{T}}$ + jets + lepton(s)] channels, where $\not{E}_{\mathrm{T}}$ stands for the missing transverse momentum carried away by the lightest supersymmetric particle (LSP). The SUSY particles masses, including that of the LSP, can be determined by exclusive studies model-independently, when a three successive two-body decay chain is identified. In more general cases, they can still be determined within various supersymmetry models.

The LHC can also discover new physics other than supersymmetry, such as new gauge boson symmetry and extra space dimensions.

1) http://lhc.web.cern.ch/lhc/
2) ATLAS technical proposal: CERN/LHCC/94-43.
3) CMS technical proposal: CERN/LHCC/94-38.
4) ATLAS Physics TDR Vol. 1, CERN/LHCC/99-15.
5) CMS Physics TDR Vol. 1, CERN/LHCC/2006-001.
6) http://lepewwg.web.cern.ch/LEPEWWG/plots/winter2007/
7) F. Wilczek: Phys. Rev. Lett. **39** (1977) 1304.
8) D. Rainwater and D. Zeppenfeld: J. High Energy Phys. **JHEP12** (1997) 005.
9) For a review, see, e.g., M. Spira: hep-ph/9705337.
10) A. Djouadi, J. Kalinowski, and M. Spira: Comput. Phys. Commun. **108** (1998) 56.
11) ATLAS Physics TDR Vol. 2, CERN/LHCC/99-15.
12) CMS Physics TDR Vol. 2, CERN/LHCC/2006-021.
13) ν is emitted along the momentum direction of the observed particles: Collinear approximation.
14) D. Rainwater, D. Zeppenfeld, and K. Hagiwara: Phys. Rev. D **59** (1998) 014037.
15) S. Asai, G. Azuelos, C. Buttar, V. Cavasinni, D. Costanzo, K. Cranmer, R. Harper, K. Jakobs, J. Kanzaki, M. Klute, R. Mazini, B. Mellado, W. Quayle, E. Richter-Was, T. Takemoto, I. Vivarelli, and S. L. Wu: Eur. Phys. J. C **32** (2002) Suppl. 2, 19.
16) For general reviews, H. P. Nilles: Phys. Rep. **110** (1984) 1; H. E. Haber and G. L. Kane: Phys. Rep. **117** (1985) 75.
17) For general reviews, G. Jungman, M. Kamionkowski, and K. Griest: Phys. Rep. **267** (1996) 195.
18) L. Alvarez-Gaumé, J. Polchinski, and M. B. Wise: Nucl. Phys. B **221** (1983) 495; L. Ibáñez: Phys. Lett. B **118** (1982) 73.
19) M. Dine, W. Fischler, and M. Srednicki: Nucl. Phys. B **189** (1981) 575; S. Dimopoulos and S. Raby: Nucl. Phys. B **192** (1981) 353.
20) L. Randall and R. Sundrum: Nucl. Phys. B **557** (1999) 79.
21) K. Hikasa and M. Kobayashi: Phys. Rev. D **36** (1987) 724.
22) E. Eichten *et al.*: Rev. Mod. Phys. **56** (1984) 579.
23) P. Fayet: Phys. Lett. B **69** (1977) 489.
24) S. Abdullin *et al.*: CMS/Note/98-006; hep-ph/9806366.
25) S. Asai: EPJ direct **4** (2002) Suppl. 1, 17.
26) B. C. Allanach, C. G. Lester, M. A. Parker, and B. R. Webber: CERN-TH-2000-149 (2000).
27) N. Arkani-Hamed, S. Dimopoulos, and G. Dvali: Phys. Lett. B **429** (1998) 263; L. Randall and R. Sundrum: Phys. Rev. Lett. **83** (1999) 3370.
28) S. Dimopoulos and G. Landsberg: Phys. Rev. Lett. **87** (2001) 161602.
29) J. Tanaka *et al.*: Eur. Phys. J. C **41** (2005) 19.

Shoji Asai was born in Ishikawa, Japan in 1967. He obtained D. Sc. (1995) degrees from the University of Tokyo. He solved the orthopositronium lifetime problem in his thesis. From 1995, Research Assistant of the University of Tokyo and his research interesting was SUSY search at LEP. From 2003, Associate Professor of the University of Tokyo. Research interests are on Physics at LHC (Susy and Higgs), and precision measurements of QED using positronium.